PHYSICAL REVIEW D **95,** 095016 (2017)

Naturalness, vacuum stability, and leptogenesis in the minimal seesaw model

Gulab Bambhaniya,[1,*] P. S. Bhupal Dev,[2,3,†] Srubabati Goswami,[1,‡] Subrata Khan,[4,5,§] and Werner Rodejohann[2,‖]

[1]*Physical Research Laboratory, Navrangpura, Ahmedabad 380009, India*

[2]*Max-Planck-Institut für Kernphysik, Saupfercheckweg 1, 69117 Heidelberg, Germany*

[3]*Department of Physics and McDonnell Center for the Space Sciences, Washington University, St. Louis, Missouri 63130, USA*

[4]*Department of Physics, University of Calcutta, Kolkata 700009, India*

[5]*Department of Physical Sciences, Indian Institute of Science Education and Research Kolkata, Mohanpur, Nadia 741246, India*

(Received 18 January 2017; published 19 May 2017)

The right-handed neutrinos within the type-I seesaw mechanism can induce large radiative corrections to the Higgs mass, and naturalness arguments can then be used to set limits on their mass scale and Yukawa couplings. Driven by minimality, we consider the presence of two degenerate right-handed neutrinos. We compare the limits from naturalness with the ones from the stability of the electroweak vacuum and from lepton flavor violation. Implications from neutrinoless double beta decay are also discussed and renormalization effects for the light neutrino parameters are presented. Adding small perturbations to the degenerate heavy neutrino spectrum allows for successful leptogenesis.

DOI: 10.1103/PhysRevD.95.095016

I. INTRODUCTION

The journey of experimentally verifying the particle content of the standard model (SM) of particle physics has finally been completed by the discovery of the Higgs boson in 2012 [1,2]. This seems to clarify the origin of masses for all standard model (SM) particles. On the other hand, the discovery of neutrino oscillations [3] and flavor conversion [4] require at least two neutrinos to be massive, which cannot be explained in the SM and necessitate the existence of new particles. It is therefore a potentially rewarding problem to investigate the connection between neutrino mass and the Higgs sector of the SM. There are indeed several possible nontrivial consequences of neutrino mass physics on the SM Higgs boson, such as

(i) *Nonstandard Higgs decays:* These could be either into new particles that are implied by models for neutrino mass or lepton mixing, or modified/new decays into SM particles; see Refs. [5–18] for some examples.

(ii) *Vacuum stability:* The couplings of the Higgs boson to new particles modify the renormalization group (RG) running of the Higgs self-coupling, and hence, the stability of the electroweak vacuum as compared to that in the SM [19]; see for instance Refs. [20–41].

(iii) *Naturalness:* Loop corrections to the Higgs mass are typically quadratic in the mass of the heaviest particle in the loop, a property responsible for the hierarchy problem. Thus, if some heavy particle responsible for neutrino mass couples to the Higgs boson, it could also lead to unacceptably large contributions to the Higgs mass. This sets an *upper* limit on the mass scale of the new particles associated to neutrino mass; see e.g. Refs. [42–51].

In this paper, we focus on the latter two aspects, and study the impact of naturalness and vacuum stability within a type-I seesaw model [52–56], where heavy right-handed neutrinos are the new particles responsible for light neutrino masses. We will study here the most minimal seesaw realization with only two heavy neutrinos [57–66]; for a review, see e.g. [67]. Thus, one light neutrino is massless at the tree level. Further assuming the masses of the heavy neutrinos to be (quasi)degenerate leaves us with 3 free parameters beyond the directly measurable light neutrino parameters, namely the mass scale of the heavy right-handed neutrinos plus one complex angle in the Casas-Ibarra (CI) parametrization [68]. We use naturalness arguments to set limits on these parameters, which mostly constrain the new mass scale and the imaginary part of the complex angle. These limits are compared with constraints from the stability of the electroweak vacuum and from lepton flavor violation (LFV). We also study the phenomenological implications of this scenario for neutrinoless double beta decay ($0\nu\beta\beta$) and the RG evolution of the light neutrino parameters. In addition, we show that the observed baryon asymmetry of the Universe (BAU) can be successfully explained, leptogenesis, for the parameter values allowed by all other constraints, if small perturbations are added to the heavy mass spectrum.

The rest of the paper is organized as follows: In Sec. II, we review the minimal seesaw model and set up our

*gulab.bambhaniya@gmail.com
†bdev@wustl.edu
‡sruba@prl.res.in
§khansubrata@gmail.com
‖werner.rodejohann@mpi-hd.mpg.de

 © 2017 American Physical Society

notation. In Sec. III, we discuss the constraints obtained on the model parameters from the naturalness criterion. In Sec. IV, we compare the naturalness constraints with those from electroweak vacuum (meta)stability and LFV. RG effects on the light neutrino parameters are studied in Sec. V. In Sec. VI, we focus on leptogenesis aspects and conclude in Sec. VII.

II. THE MINIMAL SEESAW MODEL

We consider the minimal type-I seesaw model with two heavy right-handed Majorana neutrinos N_{R_j} (with $j = 1, 2$), defined by the Lagrangian

$$-\mathcal{L} = Y_{\nu_{jl}} \bar{N}_{R_j} \tilde{\phi}^{\dagger} L_l + \frac{1}{2} \bar{N}_{R_j} M_{jk} N^c_{R_k} + \text{H.c.}, \tag{2.1}$$

where $L_l = (\nu_l, l)^T_L$ (with $l = e, \mu, \tau$) is the $SU(2)_L$ lepton doublet and $\tilde{\phi} = i\sigma_2 \phi^*$ (with σ_2 being the second Pauli matrix and $\phi = (\phi^+, \phi^0)^T$ being the SM Higgs doublet). The sum over repeated indices is implicitly assumed throughout, unless otherwise specified. We consider the scenario in which the two heavy neutrinos are degenerate so that the heavy-neutrino Majorana mass matrix is trivial: $M = \text{diag}(M_N, M_N)$. In general, the neutrino mass matrix in the (ν_L, N^c_R) basis can be written as

$$M_\nu = \begin{pmatrix} 0 & m_D^T \\ m_D & M \end{pmatrix}. \tag{2.2}$$

Here $m_D = v Y_\nu / \sqrt{2}$, where v is the vacuum expectation value (VEV) of the SM Higgs field which in our convention is defined as $\langle \phi^0 \rangle = v/\sqrt{2} = 174$ GeV. The mass matrix can be diagonalized by a 5×5 unitary matrix U_0 as

$$U_0^T M_\nu U_0 = M_\nu^{\text{diag}} = \text{diag}(m_1, m_2, m_3, M_1, M_2), \tag{2.3}$$

with mass eigenvalues m_i $(i = 1, 2, 3)$ and M_j $(j = 1, 2)$ for light and heavy neutrinos, respectively. In our case, $M_1 = M_2 = M_N$, $m_1 = 0$ for the normal hierarchy (NH), and $m_3 = 0$ for the inverted hierarchy (IH). We can write U_0 as [69–74]

$$\begin{aligned} U_0 = W U_\nu &\simeq \begin{pmatrix} (\mathbb{1} - \frac{1}{2}\epsilon) U & m_D^{\dagger} (M^{-1})^* U_R \\ -M^{-1} m_D U & (\mathbb{1} - \frac{1}{2}\epsilon') U_R \end{pmatrix} \\ &\equiv \begin{pmatrix} U_L & T \\ S & U_H \end{pmatrix}, \end{aligned} \tag{2.4}$$

where W is the matrix which block-diagonalizes the full 5×5 neutrino matrix:

$$W^T \begin{pmatrix} 0 & m_D^T \\ m_D & M \end{pmatrix} W = \begin{pmatrix} m_{\text{light}} & 0 \\ 0 & m_{\text{heavy}} \end{pmatrix}. \tag{2.5}$$

Here $U_\nu = \text{diag}(U, U_R)$ diagonalizes the mass matrices in the light and heavy sector appearing in the upper and lower block of the block diagonal matrix, respectively, in Eq. (2.5). In our case, $U_R = \mathbb{1}$ and $m_{\text{heavy}} = M$. The matrix U_L in the upper left corner of Eq. (2.4) is the new Pontecorvo-Maki-Nakagawa-Sakata (PMNS) mixing matrix, which acquires a nonunitary correction over the original PMNS matrix U, which is the matrix that diagonalizes m_{light}. Finally, ϵ and ϵ' characterize the nonunitarity and are given by

$$\begin{aligned} \epsilon &= T T^{\dagger} = m_D^{\dagger} (M^{-1})^* M^{-1} m_D, \\ \epsilon' &= S S^{\dagger} = M^{-1} m_D m_D^{\dagger} (M^{-1})^*. \end{aligned} \tag{2.6}$$

The light neutrino mass matrix, in the limit $M \gg m_D$, is given as

$$m_{\text{light}} = -m_D^T M^{-1} m_D. \tag{2.7}$$

It proves very useful to introduce the Casas-Ibarra parametrization for the Yukawa coupling matrix [68]:

$$Y_\nu = \frac{\sqrt{2}}{v} \sqrt{D_N} R \sqrt{D_\nu} U^{\dagger}, \tag{2.8}$$

where $D_N = \text{diag}(M_1, M_2)$, $D_\nu = \text{diag}(m_1, m_2, m_3)$, and R is an arbitrary 2×3 orthogonal matrix. In the minimal seesaw model, the light masses are completely fixed by the measured solar and atmospheric mass-squared differences:

$$\begin{aligned} &m_1 = 0, \quad m_2 = \sqrt{\Delta m^2_{\text{s}}}, \quad m_3 = \sqrt{\Delta m^2_{\text{a}}}, \quad \text{(NH)} \\ &m_1 = \sqrt{\Delta m^2_{\text{a}}}, \quad m_2 = \sqrt{\Delta m^2_{\text{a}} + \Delta m^2_{\text{s}}}, \quad m_3 = 0. \quad \text{(IH)} \end{aligned} \tag{2.9}$$

The matrix U in Eq. (2.8) diagonalizing the light neutrino mass matrix m_{light} is parametrized by three mixing angles θ_{ij} (with $i, j = 1, 2, 3; i \neq j$), one Dirac phase δ and one Majorana phase α:

$$U = \begin{pmatrix} c_{12}c_{13} & s_{12}c_{13} & s_{13}e^{-i\delta} \\ -s_{12}c_{23} - c_{12}s_{23}s_{13}e^{i\delta} & c_{12}c_{23} - s_{12}s_{23}s_{13}e^{i\delta} & s_{23}c_{13} \\ s_{12}s_{23} - c_{12}c_{23}s_{13}e^{i\delta} & -c_{12}s_{23} - s_{12}c_{23}s_{13}e^{i\delta} & c_{23}c_{13} \end{pmatrix} \text{diag}(e^{-i\alpha}, e^{+i\alpha}, 1), \tag{2.10}$$

where $c_{ij} \equiv \cos\theta_{ij}$, $s_{ij} \equiv \sin\theta_{ij}$. For numerical purposes, we will use the 3σ ranges of the mass-squared differences and mixing parameters from the global-fit of Ref. [75] and vary the CP phases δ and α between $-\pi$ to $+\pi$, unless otherwise specified.

From Eq. (2.8) we have

$$R_{ij} = \frac{(Y_\nu U)_{ij}}{\sqrt{M_i m_j}} \frac{v}{\sqrt{2}}, \tag{2.11}$$

where $j \neq 1$ for NH and $j \neq 3$ for IH. We can parametrize the matrix R as

$$R = \begin{cases} \begin{pmatrix} 0 & \cos z & \zeta \sin z \\ 0 & -\sin z & \zeta \cos z \end{pmatrix} & \text{(NH)} \\ \begin{pmatrix} \cos z & \zeta \sin z & 0 \\ -\sin z & \zeta \cos z & 0 \end{pmatrix} & \text{(IH)}. \end{cases} \tag{2.12}$$

Here z is a complex parameter and $\zeta = \pm 1$, which however has no influence for our results; so we will use $\zeta = +1$ from now on.

III. CONSTRAINTS FROM NATURALNESS

We will discuss in this section the implications of the type-I seesaw from naturalness; see also Refs. [42,46]. The potential of the SM Higgs boson at tree level can be written as

$$V = -\mu^2(\phi^\dagger\phi) + \lambda(\phi^\dagger\phi)^2, \tag{3.1}$$

from which the physical Higgs mass is given as $m_h^2 = 2\lambda v^2$. Heavy right-handed neutrino loop corrections to the electroweak μ parameter are desired to be smaller than $\mathcal{O}(\text{TeV}^2)$ for naturalness of the Higgs mass. The relevant diagram is shown in Fig. 1. Using the $\bar{\text{MS}}$ scheme and taking the quantity $(\ln[\frac{M_j}{\mu_R}] - \frac{1}{2})$ to be unity (where μ_R is the renormalization scale), the correction is given as

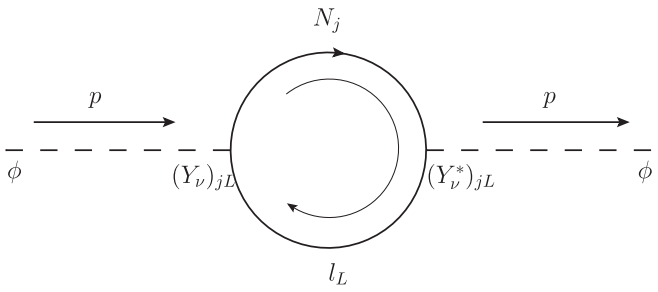

FIG. 1. One-loop correction to the Higgs mass from neutrino Yukawa couplings due to the heavy neutrinos. The line inside the loop shows the orientation of lepton number.

$$\delta\mu^2 \approx \frac{1}{4\pi^2} \text{Tr}[Y_\nu^\dagger D_N^2 Y_\nu]. \tag{3.2}$$

Now using the CI parametrization from Eq. (2.8), we get the simple relation

$$\delta\mu^2 \approx \frac{1}{4\pi^2}\frac{2}{v^2}\text{Tr}[D_\nu R^\dagger D_N^3 R] = \frac{M_N^3}{2\pi^2 v^2}\cosh(2\text{Im}[z]) \times \begin{cases} (m_2 + m_3) & \text{(NH)} \\ (m_1 + m_2) & \text{(IH)} \end{cases} \tag{3.3}$$

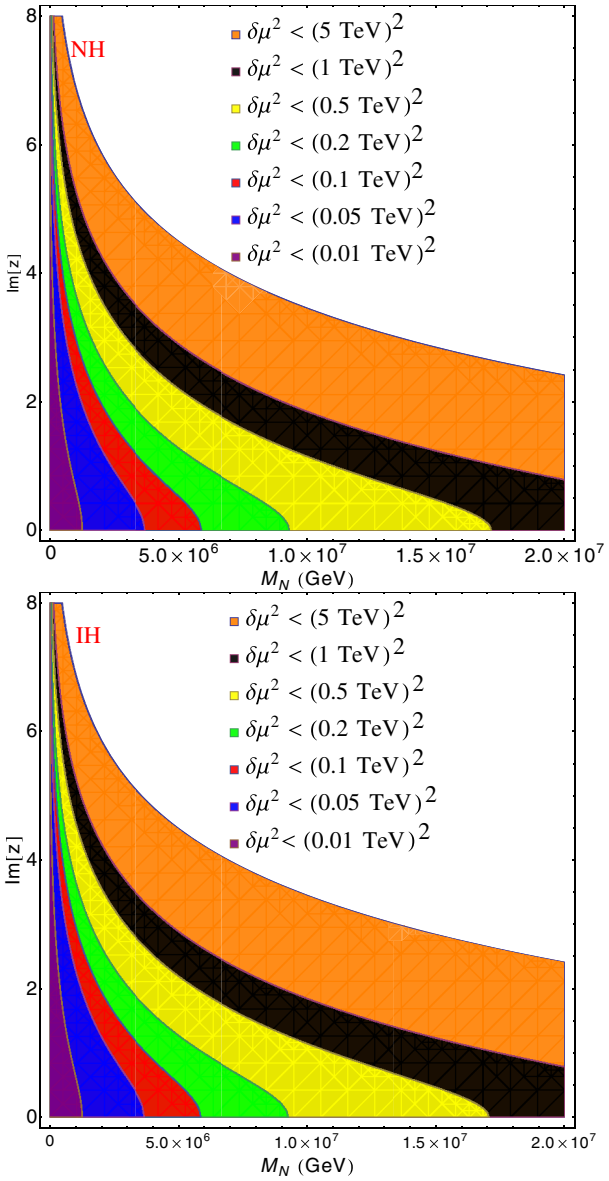

FIG. 2. Naturalness contours in the Im[z]–M_N plane. The left (right) plot is for NH (IH). In the colored shaded regions, $\delta\mu^2$ is demanded to be below (p% of 1 TeV)^2, where $p = 500, 100, 50, 20, 10, 5, 1$ (from top to bottom). The unshaded regions are disfavored by naturalness.

Note that the real part of the complex angle z in the CI parametrization does not appear in Eq. (3.3). The PMNS mixing angles and CP phases also drop out in this expression. In the following discussion, the only relevant free parameters will therefore be M_N and Im$[z]$. Also note that for a given choice of Im$[z]$, the correction in case of NH is about half the size of that in IH.

In Fig. 2 we show the regions in the Im$[z]$–M_N plane corresponding to different upper limits of $\delta\mu^2$ ranging from $(5\ \text{TeV})^2$ down to $(0.01\ \text{TeV})^2$ for both NH and IH. The areas to the right of the shaded regions are thus disfavored from the condition of naturalness. From Fig. 2, we see that the larger Im$[z]$ is, the smaller the allowed value of M_N becomes. For instance, demanding $\delta\mu^2 < (1\ \text{TeV})^2$ implies $M_N < 2.7 \times 10^7$ GeV for Im$[z] = 0$ and $M_N < 1.2 \times 10^6$ GeV for Im$[z] = 5$. Similarly, demanding $\delta\mu^2 < (0.01\ \text{TeV})^2$ implies $M_N < 1.2 \times 10^6$ GeV for Im$[z] = 0$ and $M_N < 5.6 \times 10^4$ GeV for Im$[z] = 5$. In what follows, we will often use characteristic example values, corresponding to the maximal values of Im$[z]$ for a given M_N. These are, for $\delta\mu^2 < (1\ \text{TeV})^2$, Im$[z] = 8.75$ at $M_N = 10^5$ GeV and Im$[z] = 11.17$ at $M_N = 2 \times 10^4$ GeV.

We should mention here that the naturalness constraints discussed above could in principle be relaxed if nature was supersymmetric at some scale below $\sim 10^7$ GeV. For instance, there are additional corrections to the Higgs mass from sneutrino loops which could in principle cancel those from RH neutrinos, if they have similar masses. However, we do not discuss this possibility here, simply because we are driven here by the minimality of the seesaw model.

IV. COMPARISON WITH OTHER BOUNDS

In this section we compare the constraints from naturalness obtained in Sec. III with those obtained from metastability of the electroweak vacuum (see Sec. IV A) and with phenomenological limits arising from LFV (see Sec. IV B). We also discuss implications for lepton number violating processes, such as $0\nu\beta\beta$ (see Sec. IV C).

A. Bounds from metastability

We discuss in this section the constraints on the Yukawa coupling Y_ν and the heavy neutrino mass M_N arising from metastability of the electroweak vacuum. The relevant RG equations can be found, e.g. in Refs. [28,40] and are not repeated here. We just note here that the RG equations depend on the quantities

$$\text{Tr}(Y_\nu^\dagger Y_\nu) = \frac{2}{v^2}\text{Tr}[R^\dagger D_N R D_\nu] = \frac{2}{v^2} M_N \cosh(2\text{Im}[z]) \times \begin{cases} (m_2 + m_3) & \text{(NH)} \\ (m_1 + m_2) & \text{(IH)} \end{cases} \tag{4.1}$$

$$\text{Tr}(Y_\nu^\dagger Y_\nu Y_\nu^\dagger Y_\nu) = \frac{4}{v^4}\text{Tr}[(R^\dagger D_N R D_\nu)^2] = \frac{4}{v^4} M_N^2 \times \begin{cases} [(m_2^2 + m_3^2)\cosh^2(2\text{Im}[z]) + 2m_2 m_3 \sinh^2(2\text{Im}[z])] & \text{(NH)} \\ [(m_1^2 + m_2^2)\cosh^2(2\text{Im}[z]) + 2m_1 m_2 \sinh^2(2\text{Im}[z])] & \text{(IH)} \end{cases} \tag{4.2}$$

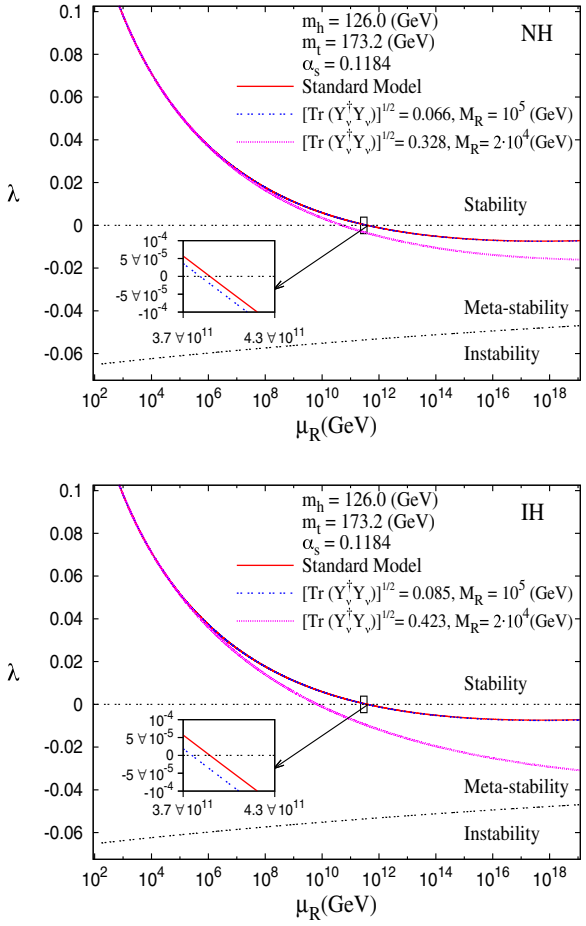

FIG. 3. Running of the SM Higgs quartic coupling λ for NH (left panel) and IH (right panel) in the minimal seesaw model. The red solid line corresponds to the SM running, while the blue dotted line corresponds to the SM + heavy neutrino contribution for $M_N = 10^5$ GeV. For this mass $(\text{Tr}[Y_\nu^\dagger Y_\nu])^{1/2} = 0.066$ is small and hence it almost overlaps with the SM line. In the inset both lines are shown with magnified view. For $M_N = 2 \times 10^4$ GeV the maximal allowed trace value is larger, $(\text{Tr}[Y_\nu^\dagger Y_\nu])^{1/2} = 0.328$, hence the effect is sizable and the corresponding pink line is visibly separated from the SM one.

In Fig. 3 we show the running of the quartic coupling λ as a function of the renormalization scale μ_R. We have chosen here and in the following the Higgs mass $m_h = 126$ GeV, the top quark mass $m_t = 173.2$ GeV and the strong coupling constant as $\alpha_s = 0.1184$ at the electroweak scale. The dashed horizontal line in Fig. 3 shows the absolute stability condition for the vacuum, i.e. $\lambda > 0$ for all μ_R. While for sizable part of parameter space $\lambda < 0$ is reached, it is however possible to find regions where the vacuum is metastable, i.e., the lifetime of the vacuum remains higher than the age of the Universe. Adopting a semiclassical approach, the tunneling probability at zero temperature can be written as [76–79]

$$p = \max_{\mu<\Lambda} V_U \mu^4 \exp\left(-\frac{8\pi^2}{3|\lambda(\mu)|}\right), \tag{4.3}$$

where Λ denotes the cutoff scale and V_U represents the volume of the past light-cone which goes as τ^4, with $\tau = 4.35 \times 10^{17}$ sec being the age of the Universe [80]. Metastability of the vacuum implies $p < 1$, which in turn puts a lower bound on λ as

$$|\lambda| < \lambda^{\max}_{\text{meta}} = \frac{8\pi^2}{3}\frac{1}{4\ln(\tau\mu)}. \tag{4.4}$$

We choose μ in Eq. (4.3) as the scale at which λ becomes most negative. This constraint is shown by the slanting dashed line in Fig. 3.

The red solid line in Fig. 3 shows the running of λ in the SM. The blue dashed line and the pink solid line show the running of this quantity in the minimal seesaw model considered here for two representative values of M_N. The blue dashed line is for $M_N = 10^5$ GeV for which the maximum value of Im$[z]$ allowed by naturalness is 8.75 [cf. Fig. 2 and Eq. (4.1)]. With this value of Im$[z]$, $(\text{Tr}[Y_\nu^\dagger Y_\nu])^{1/2}$ is found to be 0.085 and results only in a small difference with respect to the running in the SM. In the inset we show a magnified version of the region in μ_R where the stability limit is crossed for the SM and the minimal seesaw cases. It is clear from the inset that the stability is lost at a lower renormalization scale for the minimal seesaw model. The pink solid line shows the running of λ for a lower value of $M_N = 2 \times 10^4$ GeV. This implies a higher maximum allowed value of Im$[z] = 11.17$ for both NH and IH, and hence, implies a larger $(\text{Tr}[Y_\nu^\dagger Y_\nu])^{1/2} = 0.423$. In this case the difference with respect to the SM running is clearly visible and the stability is lost earlier. However, in both cases the metastability bound remains satisfied.

The metastability condition can be used to impose an upper bound on $\text{Tr}[Y_\nu^\dagger Y_\nu]$ from the running of λ as a function of the heavy neutrino mass M_N. This is shown by the red-dashed line in Fig. 4 for both NH (left) and IH (right). The area below this curve is allowed from the metastability condition. This figure also shows the allowed region satisfying the condition of perturbativity $(\text{Tr}[Y_\nu^\dagger Y_\nu] \leq 4\pi)$, which is shown by the green solid line. The perturbativity bound is seen to be weaker than the metastability bound. For comparison, we also show the bound obtained from the naturalness criterion $\delta\mu^2 < (p\ \text{TeV})^2$ with $p = 5$, 1, 0.2, as shown by the orange, blue and pink dotted lines respectively, where the area to the left of these lines is preferred by naturalness. Figure 4 also contains bounds coming from LFV considerations (see Sec. IV B). Figure 5 shows the same constraints in the parameter space of Im$[z]$ and M_N.

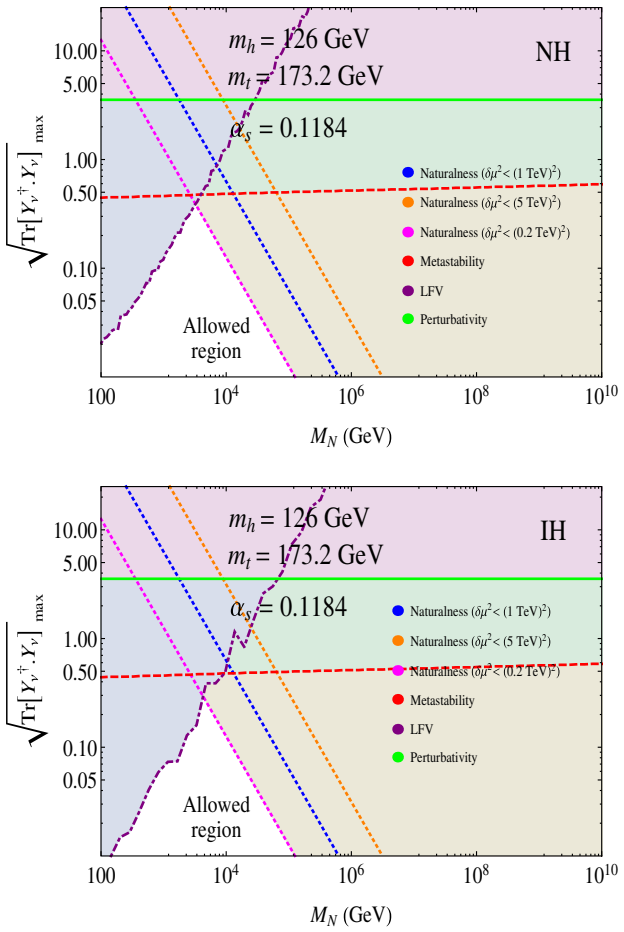

FIG. 4. Bounds on $(\text{Tr}[Y_\nu^\dagger Y_\nu])^{1/2}$ from metastability (red dashed), naturalness (blue dotted), LFV (dark red dot-dashed) and perturbativity (green solid).

We find that for heavy neutrino masses larger than about 10^4 GeV, naturalness provides the strongest constraint on the minimal seesaw scenario.

B. Lepton flavor violation

The strongest LFV bound on the minimal seesaw scenario comes from the branching ratio for muon decay, $\mu \to e\gamma$, which is given by [81–83]

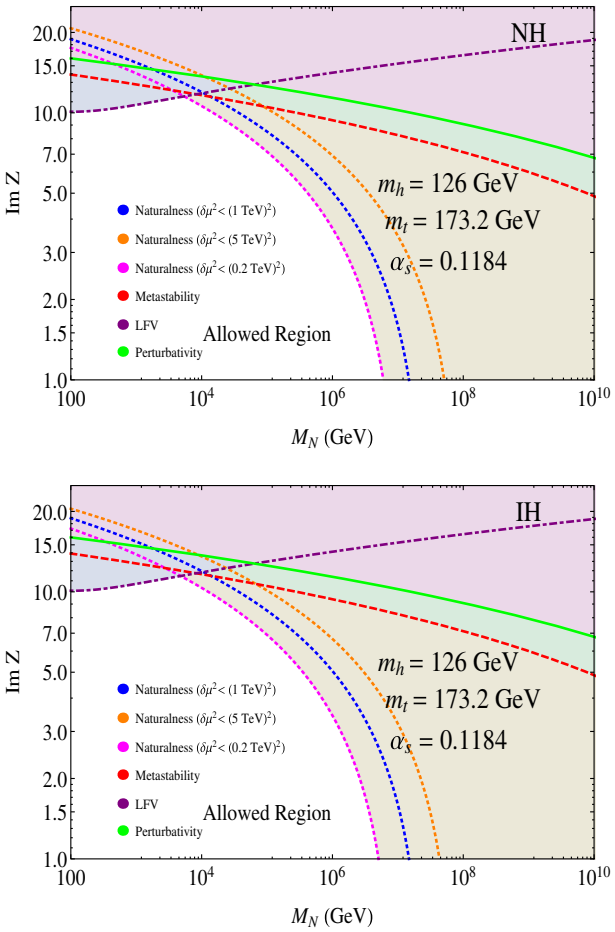

FIG. 5. Bounds on Im$[z]$ as a function of M_N, with the same notation as in figure 4.

$$\text{Br}(\mu \to e\gamma) = \frac{3\alpha_e}{8\pi}|T_{ei}T^{\dagger}_{i\mu}f(x_i)|^2, \tag{4.5}$$

where $\alpha_e \equiv e^2/4\pi$ is the fine-structure constant, $x_i = (\frac{M_i^2}{m_W^2})$ and

$$f(x) = \frac{x(1-6x+3x^2+2x^3-6x^2\ln x)}{2(1-x)^4} \tag{4.6}$$

is a slowly varying function of x ranging from 0 to 1 for $x \in [0,\infty]$. The elements of the matrix T denote the light-heavy mixing which is responsible for the nonunitarity of the lepton mixing matrix. In our scenario, $T = m_D^{\dagger}(M^{-1})^* U_R$ [cf. Eq. (2.4)], and m_D is given in terms of the CI parametrization which introduces a dependence on the PMNS matrix. The result for $|T_{ei}T^{\dagger}_{i\mu}|^2$ is a lengthy expression including the PMNS matrix elements, light and heavy neutrino masses, as well as z, which is solved numerically. The resulting branching ratio has to be confronted with the latest experimental limit [84] of

$$\text{Br}(\mu \to e\gamma) < 4.2 \times 10^{-13}. \tag{4.7}$$

The LFV constraints on Im$[z]$ and M_N, are displayed in Fig. 5. In obtaining this, we vary the light neutrino mass and mixing parameters within their 3σ allowed range, the phases in the range $0-2\pi$ and take the extreme value that gives maximum disallowed region. The constraints on z can be translated into constraints on $\text{Tr}([Y_\nu^{\dagger}Y_\nu])^{1/2}$ [cf. Eq. (4.1)], which are shown in Fig. 4. Comparing with the naturalness, metastability and perturbativity constraints, we find that in the case of NH, LFV provides the strongest limits for relatively small heavy neutrino masses up to $M_N \sim 1$ TeV, then metastability takes over for a short mass range, before naturalness imposes the strongest constraint on the minimal seesaw scenario. In the IH case, the situation is very similar, but for a given M_N, the constraint from LFV on the Yukawa couplings is slightly stronger in the IH case than in the NH case. This can be understood from the expression $x_{e\mu} \equiv |T_{ei}T^{\dagger}_{i\mu}|^2$, which is larger for the IH case. In order to see it analytically, the lengthy formulas can be shortened in the limit of $\sin^2\theta_{13} = 0$, $\sin^2\theta_{23} = \frac{1}{2}$ and $\sin^2\theta_{12} = \frac{1}{3}$, and one finds

$$x_{e\mu}^{\text{NH}} \approx \frac{2\Delta m_{\text{a}}^2}{M_N^2}(\cosh^2(2\text{Im}[z])), \tag{4.8}$$

$$x_{e\mu}^{\text{IH}} \approx \frac{2\Delta m_{\text{a}}^2}{M_N^2}\left(\sinh^2(2\text{Im}[z]) + \frac{1}{9}\cosh^2(2\text{Im}[z])\right), \tag{4.9}$$

which illustrates that $x_{e\mu}$ is typically larger in the IH case for Im$[z] \gtrsim 1$.

C. Neutrinoless double beta decay

Surprisingly, even for rather low values of the right-handed neutrino masses, neutrinoless double beta decay $(0\nu\beta\beta)$ [85] does not provide significant constraints in our scenario. The half-life for $0\nu\beta\beta$ in presence of heavy Majorana neutrinos is given by (see e.g. Refs. [86–91])

$$\frac{1}{T_{1/2}^{0\nu}} = G\frac{|\mathcal{M}_\nu|^2}{m_e^2}\left|U_{ei}^2 m_i + \langle p^2\rangle\frac{T_{ei}^2}{M_i}\right|^2, \tag{4.10}$$

where G denotes the phase space factor and $\langle p^2\rangle = -m_e m_p \mathcal{M}_N/\mathcal{M}_\nu$, whose magnitude is typically of order $(100\ \text{MeV})^2$. Here $\mathcal{M}_\nu$ and $\mathcal{M}_N$ denote the nuclear matrix elements corresponding to light and heavy neutrino exchange, respectively. Using the general expression of $T = m_D^{\dagger}(M^{-1})^* U_R$ from Eq. (2.4) and Y_ν from Eq. (2.8), we can write $\sum_i T_{ei}^2/M_i = \sum_i U_{ei}^2 m_i/M_N^2$, where M_N is the degenerate heavy neutrino mass. Substituting this in Eq. (4.10), we find that the heavy-neutrino exchange contribution is suppressed by a factor of $\langle p^2\rangle/M_N^2$, as compared to the light neutrino exchange contribution; see

also Refs. [92–94]. For heavy neutrino masses even as low as 100 GeV, the contribution of those to the $0\nu\beta\beta$ half-life is therefore negligible. The contribution of light neutrinos is given by the usual expressions for a vanishing smallest neutrino mass, see e.g. Ref. [85].

We should note here that electroweak-scale heavy neutrinos in the minimal seesaw can also be constrained from the LHC data using either the same-sign dilepton plus dijet channel (for scenarios with large lepton number violation) or opposite-sign dilepton or trilepton channels (for suppressed lepton number violation); for a review, see e.g. [95]. However, the current collider constraints turn out to be weaker than the other constraints shown in Fig. 4 for the range of heavy neutrino masses considered here.

V. RUNNING OF LIGHT NEUTRINO PARAMETERS

In this section we discuss the RG evolution effect on light neutrino parameters in the context of the natural seesaw scenario considered in this work. We follow the procedure described in Ref. [96].

Starting with low energy parameters, the running of light neutrino parameters [97] is governed by the effective dimension-5 operator

$$\mathcal{L}_{\rm eff} = \frac{1}{4}(\overline{l_L^C}\epsilon\phi)\kappa(\phi^T\epsilon^T l_L) + \text{H.c.}, \tag{5.1}$$

where $\kappa = 2Y_\nu^T M_R^{-1} Y_\nu = 4m_\nu/v^2$. When the energy scale of the heavy neutrino masses is reached, different RG equations of the full renormalizable theory have to be considered [98], and threshold effects can be important. We solve the evolution equations numerically taking into account the threshold effect at the mass scale of the degenerate neutrinos. In our analysis for this subsection, we take $M_N = 1.32 \times 10^4$ GeV for which the maximum allowed value of Im$[z]$ is 11.797(11.544) for NH (IH).

Figure 6 shows the running of the solar and atmospheric mass-squared differences $\Delta m_s^2 \equiv m_2^2 - m_1^2$ and $\Delta m_a^2 \equiv m_3^2 - m_2^2$ for NH and $m_1^2 - m_3^2$ for IH. The figures show that the mass parameters do not run much. This is expected since the running of the masses is proportional to the masses themselves and it is well known that for hierarchical neutrinos the running is not very significant [97].

Figure 7 shows the running of the mixing angle $\sin^2\theta_{12}$ for NH and IH. Note that due to the presence of threshold effects the running is not unidirectional and while running from low to high scale the value of the mixing angle can either increase or decrease [96]. The figure shows the maximum running of this angle in both directions by

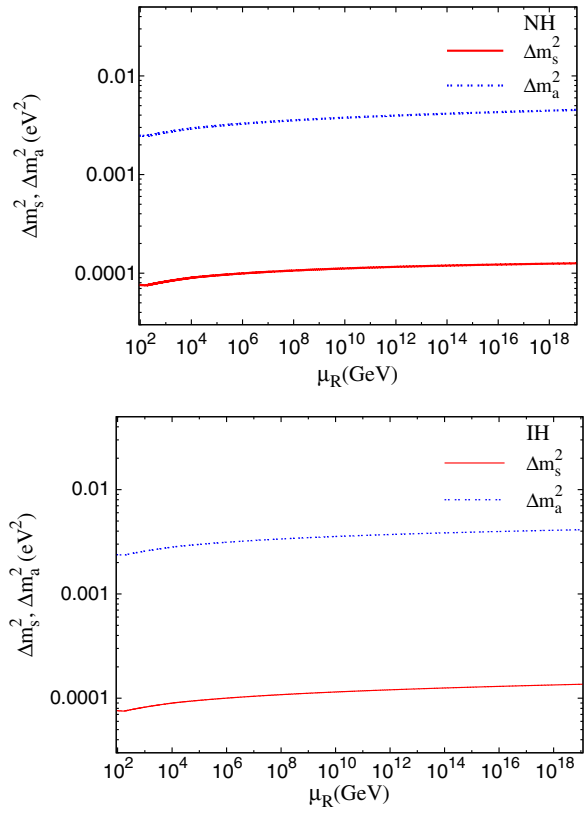

FIG. 6. Running of solar and atmospheric mass-squared differences with the renormalization scale. The plots correspond to the central values of the oscillation parameters, the Majorana phase is chosen to be $\pi/4$.

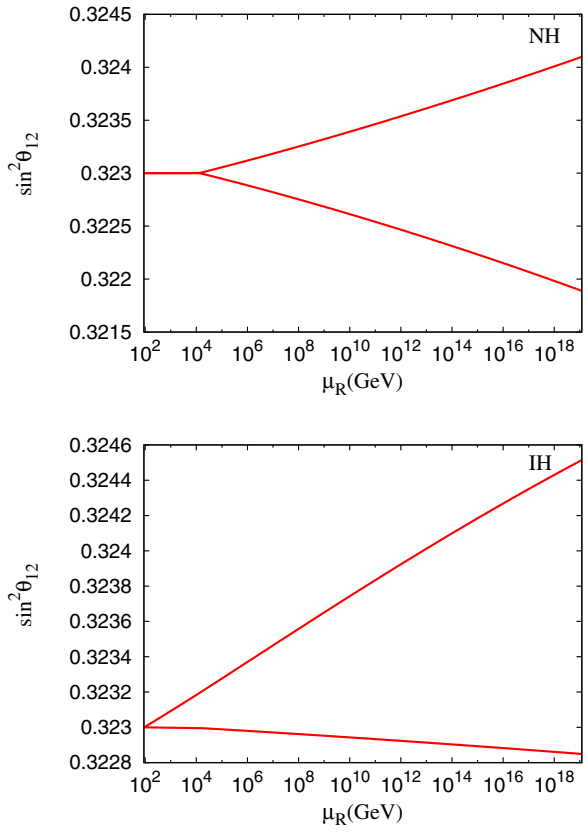

FIG. 7. Running of $\sin^2\theta_{12}$ with the renormalization scale for NH and IH. The plots correspond to the central value of $\sin^2\theta_{12}$, all other parameters are varied in their 3σ ranges.

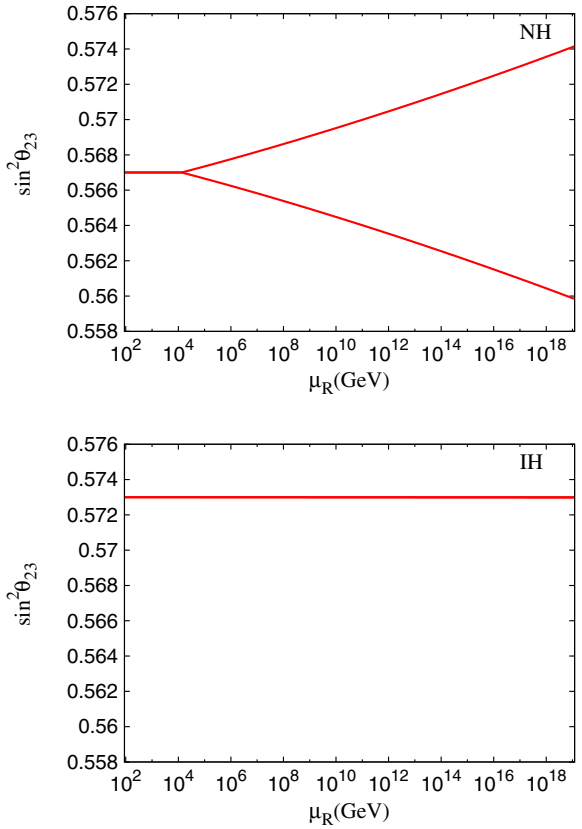

FIG. 8. Running of $\sin^2\theta_{23}$ with the renormalization scale for NH and IH. The plots correspond to the central value of $\sin^2\theta_{23}$, all other parameters are varied in their 3σ ranges.

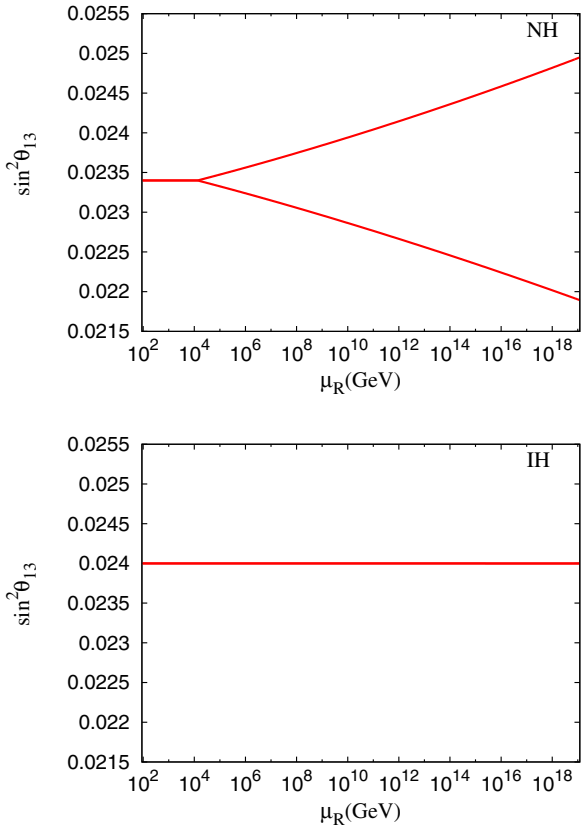

FIG. 9. Running of $\sin^2\theta_{13}$ with the renormalization scale for NH and IH. The plots correspond to the central value of $\sin^2\theta_{13}$, all other parameters are varied in their 3σ ranges.

varying all the oscillation parameters in their allowed 3σ range and both CP phases in the range $-\pi$ to $+\pi$. It is seen that although the high-scale value can be lower or higher than the low scale value the dispersion due to RG effects is not large.

Figure 8 shows the running of the mixing angle $\sin^2\theta_{23}$ for NH and IH. We take the low scale value to be in the higher octant, $\theta_{23} > \pi/4$. The running for NH can be in both directions due to the threshold effect and we show the maximum and minimum amount of running obtained by varying the parameters in their 3σ ranges. Note that even after running, the octant does not change between low and high scale. For IH, $\sin^2\theta_{23}$ does not run as the running is proportional to m_3 which is zero in our model. This is also true for $\sin^2\theta_{13}$ and this is reflected in the right plot of Fig. 9 which shows the running of $\sin^2\theta_{13}$ for IH. For NH, again due to threshold effects the high scale value can be lower or higher than the low-scale value.

The RG running discussed above will be somewhat modified for the nondegenerate and/or 3 RH neutrino case. However, we expect our results to be valid to, say 0.005 eV for the smallest neutrino mass, beyond which typical enhancement factors of RG running as in Table 2 of Ref. [97] will apply. Making the RH neutrinos nondegenerate makes the RG running essentially unpredictable unless one specifies exactly their masses. This also takes us beyond the minimality, which is the main topic of this paper.

VI. LEPTOGENESIS

A cosmological consequence of the type-I seesaw mechanism is that the CP-violating decays of the heavy Majorana neutrinos can explain the observed BAU by the mechanism of leptogenesis [99]. However, the naturalness and other constraints discussed in Sec. IV (see Fig. 5) disfavor [46] standard thermal leptogenesis, which requires $M_N \gtrsim 10^9$ GeV [100,101]. As we will show in this section, resonant leptogenesis (RL) [102–104] is a viable alternative to explain the observed BAU in the minimal natural seesaw.

In the RL mechanism, a small mass splitting ΔM_N between the two heavy neutrinos of the order of their average decay width Γ_N leads to the resonant enhancement of the ε-type CP asymmetry [103]. A minimal way to motivate the quasidegeneracy between the heavy neutrinos is by radiative effects [105–107], starting from a degenerate spectrum at some high scale [108–110]. However, this minimal scenario is not viable here, as the leptonic CP asymmetry vanishes identically at $\mathcal{O}(Y_\nu^4)$ [111]. To avoid this no-go theorem, one needs to include a new source of

flavor breaking mass splitting in the heavy-neutrino sector, which could in principle be motivated from the approximate breaking of some flavor symmetry in the leptonic sector. Here we simply assume this to be the case and choose the mass splitting $\Delta M_N \simeq \Gamma_N/2$ to maximize the CP asymmetry, without investigating the details of how this could be generated in a concrete flavor model. The only relevant effect of this small splitting is within leptogenesis.

The flavored CP asymmetry due to heavy-neutrino mixing is given by (see e.g. Ref. [110])

$$\varepsilon_{il}^{\rm mix} = \sum_{j\neq i} \frac{{\rm Im}[Y_{\nu_{il}} Y^*_{\nu_{jl}} (Y_\nu Y_\nu^\dagger)_{ij}] + \frac{M_i}{M_j} {\rm Im}[Y_{\nu_{il}} Y^*_{\nu_{jl}} (Y_\nu Y_\nu^\dagger)_{ji}]}{(Y_\nu Y_\nu^\dagger)_{ii} (Y_\nu Y_\nu^\dagger)_{jj}} f_{ij}^{\rm mix}, \tag{6.1}$$

with the regulator given by

$$f_{ij}^{\rm mix} = \frac{(M_i^2 - M_j^2) M_i \Gamma_j}{(M_i^2 - M_j^2)^2 + M_i^2 \Gamma_j^2}, \tag{6.2}$$

where $\Gamma_i = (M_i/8\pi)(Y_\nu Y_\nu^\dagger)_{ii}$ is the tree-level heavy-neutrino decay width. There is a similar contribution $\varepsilon_{il}^{\rm osc}$ to the CP asymmetry from heavy-neutrino oscillations [110,112], which is formally at $\mathcal{O}(Y_\nu^4)$, different from the $\mathcal{O}(Y_\nu^6)$ effect for GeV-scale seesaw as considered in Refs. [113–115]. Its form is given by Eq. (6.1) with the replacement $f_{ij}^{\rm mix} \to f_{ij}^{\rm osc}$, where [110,112]

$$f_{ij}^{\rm osc} = \frac{(M_i^2 - M_j^2) M_i \Gamma_j}{(M_i^2 - M_j^2)^2 + (M_i\Gamma_i + M_j\Gamma_j)^2 \frac{\det[{\rm Re}(Y_\nu Y_\nu^\dagger)]}{(Y_\nu Y_\nu^\dagger)_{ii}(Y_\nu Y_\nu^\dagger)_{jj}}}. \tag{6.3}$$

The total CP asymmetry is thus given by $\varepsilon_{il} = \varepsilon_{il}^{\rm mix} + \varepsilon_{il}^{\rm osc}$.

After solving the relevant flavored Boltzmann equations and taking into account the appropriate efficiency and dilution factors (for details, see e.g. Refs. [109,110,116]), the final BAU $\eta_B \equiv n_B/n_\gamma$ (where n_B, n_γ are the number densities of baryons and photons today) can be written analytically as

$$\eta_B \simeq -\frac{28}{51}\frac{1}{27}\frac{3}{2} \sum_{l,i} \frac{\varepsilon_{il}}{K_l^{\rm eff} \min(z_c, z_l)}, \tag{6.4}$$

where $z_c = M_N/T_c$, $T_c \sim 149$ GeV being the critical temperature below which the sphaleron transition processes freeze-out [117,118], $z_l \simeq 1.25 \log(25 K_l^{\rm eff})$ [109] and

$$K_l^{\rm eff} = \kappa_l \sum_i K_i B_{il}. \tag{6.5}$$

Here the K-factors are defined by $K_i = \Gamma_i/H_N$, where $H_N = 1.66\sqrt{g_*} M_N^2/M_{\rm Pl}$ is the Hubble rate at temperature $T = M_N$, $M_{\rm Pl} = 1.22 \times 10^{19}$ GeV is the Planck mass and $g_* \simeq 106.75$ are the relativistic degrees of freedom at that temperature. In Eq. (6.5), B_{il}'s are the branching ratios of the N_i decay to leptons of the lth flavor: $B_{il} = |Y_{\nu_{il}}|^2/(Y_\nu Y_\nu^\dagger)_{ii}$. Finally, the κ-factor in Eq. (6.5) includes the effect of the real intermediate state subtracted collision terms:

$$\kappa_l = 2 \sum_{i,j(j\neq i)} \frac{{\rm Re}[Y_{\nu_{il}} Y^*_{\nu_{jl}} (YY^\dagger)_{ij}] + {\rm Im}[(Y_{\nu_{il}} Y^*_{\nu_{jl}})^2]}{{\rm Re}[(Y^\dagger Y)_{ll}\{(YY^\dagger)_{ii} + (YY^\dagger)_{jj}\}]} \times \left(1 - 2i\frac{M_i - M_j}{\Gamma_i + \Gamma_j}\right)^{-1}. \tag{6.6}$$

Using Eq. (6.4) and the CI parametrization (2.8) for the Yukawa couplings, we calculate the BAU as a function of the average heavy-neutrino mass and the CI parameter ${\rm Im}[z]$. Here we have assumed ${\rm Re}[z] = 0$ for simplicity, since the naturalness discussion is unaffected by this choice. The result is shown in Fig. 10 for NH. The brown shaded region cannot reproduce the BAU within 3σ of the measured value: $\eta_B^{\rm obs} = (6.04 \pm 0.08) \times 10^{-10}$ [80], either in magnitude or in sign, and is therefore disfavored. On the other hand, in the white region below it, there always exists a suitable combination of the hitherto unknown CP phases δ and α (see Fig. 11 below) which can reproduce the observed BAU. Note that the BAU constraint is almost independent of ${\rm Im}[z]$ for $M_N \gtrsim 1$ TeV. For lower masses closer to the electroweak scale, the observed asymmetry requires a larger value of ${\rm Im}[z]$. As we go below the critical temperature T_c for sphaleron transitions, the conversion efficiency for the lepton-to-baryon asymmetry drops exponentially.

Comparing this result with the other constraints shown in Fig. 5, we find that the leptogenesis constraints are more

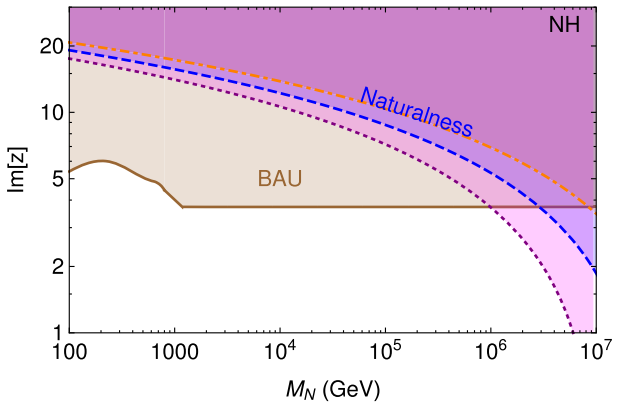

FIG. 10. Leptogenesis constraints on the minimal seesaw parameter space. The region above the brown shaded region cannot reproduce the correct BAU (either in magnitude or in sign). For comparison, the naturalness constraints [cf. Fig. 5] are also shown for $\delta\mu^2 < (p\ {\rm TeV})^2$, where $p = 5$ (orange), 1 (blue) and 0.2 (magenta), the shaded regions being disfavored.

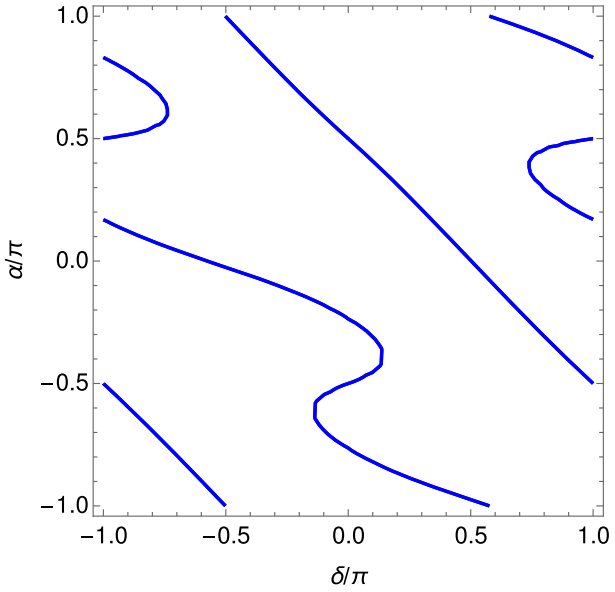

FIG. 11. Contours of the correct BAU as a function of the low energy *CP* phases. Here we have fixed $M_N = 1$ TeV and $\mathrm{Im}[z] = 0.3$.

stringent up to $M_N \lesssim 2 \times 10^6$ GeV, beyond which the naturalness constraint $\delta\mu^2 < (1\ \mathrm{TeV})^2$ (which excludes the blue shaded region) takes over. For smaller (larger) values of $(\delta\mu^2)_{\mathrm{max}}$, the naturalness constraint will be stronger (weaker), as illustrated in Fig. 10 for $\delta\mu^2 < (p\ \mathrm{TeV})^2$ with $p = 0.2$ (magenta) and 5 (orange), respectively.

To illustrate the point that in the unshaded region of Fig. 10, there always exists a suitable combination of the *CP* phases to reproduce the correct BAU, we have plotted the contours of correct BAU as a function of these phases in Fig. 11. Here we have fixed $M_N = 1$ TeV, $\mathrm{Im}[z] = 0.3$ and the other PMNS parameters at their NH best-fit values for illustration. Similar plots can be produced for any other allowed values of M_N and $\mathrm{Im}[z]$. Note that a future measurement of the Dirac *CP* phase δ with sufficient precision would imply that for a given set of values for the minimal seesaw parameters M_N and $\mathrm{Im}[z]$, there exist only a finite number of choices for the Majorana phase α that could explain the observed BAU. One can derive similar conclusions for the IH case.

VII. CONCLUSION

We have studied the implications of naturalness on the parameter space of a minimal type-I seesaw model. We have considered two degenerate heavy right-handed neutrinos and evaluated their correction to the Higgs mass parameter, obtaining thereby naturalness constraints on the heavy neutrino mass and Yukawa couplings. We have compared these bounds with constraints stemming from the stability of the electroweak vacuum. Lepton flavor violation constraints from the decay $\mu \to e\gamma$ are also important for heavy neutrino masses below TeV range, whereas naturalness provides stronger constraints for masses above 10^4 GeV or so. Metastability provides important limits in the intermediate regime.

In the allowed parameter space we have furthermore studied the effect on the RG evolution of neutrino mass and mixing parameters. Although the running shows the hallmark of threshold effects with some of the mixing angles showing bidirectional running from low to high scale depending on the parameters, in general due to the hierarchical nature of the light mass spectrum the running is not very significant.

We have also discussed the possibility of successful leptogenesis in this model. This is achieved by introducing a small mass splitting between the two heavy neutrinos comparable to their decay width. In this scenario, we find that leptogenesis provide the most stringent constraints for heavy neutrino masses below 10^6 GeV or so, while naturalness constraints are stronger for higher masses.

The model considered here represents the most economic seesaw scenario in terms of particle content that can be consistent with observed neutrino masses in oscillation experiments, naturalness, metastability of the electroweak vacuum, lepton flavor violation and leptogenesis.

ACKNOWLEDGMENTS

We thank Serguey Petcov and Branimir Radovčić for helpful comments and discussions. B. D. was supported in part by the DFG Grant No. RO 2516/5-1. S. K. was supported in part by UGC Dr. D. S. Kothari Postdoctoral Fellowship Grant No. F.4-2/2006(BSR)/PH/14-15/0117. W. R. was supported by the DFG in the Heisenberg Programme with Grant No. RO 2516/6-1.

[1] G. Aad *et al.* (ATLAS Collaboration), Phys. Lett. B **716**, 1 (2012).
[2] S. Chatrchyan *et al.* (CMS Collaboration), Phys. Lett. B **716**, 30 (2012).
[3] T. Kajita, Rev. Mod. Phys. **88**, 030501 (2016).
[4] A. B. McDonald, Rev. Mod. Phys. **88**, 030502 (2016).
[5] G. Bhattacharyya, P. Leser, and H. Pas, Phys. Rev. D **83**, 011701 (2011).
[6] P. S. B. Dev, R. Franceschini, and R. N. Mohapatra, Phys. Rev. D **86**, 093010 (2012).

[7] C. G. Cely, A. Ibarra, E. Molinaro, and S. T. Petcov, Phys. Lett. B **718**, 957 (2013).
[8] P. Bandyopadhyay, E. J. Chun, H. Okada, and J.-C. Park, J. High Energy Phys. 01 (2013) 079.
[9] S. Banerjee, P. S. B. Dev, S. Mondal, B. Mukhopadhyaya, and S. Roy, J. High Energy Phys. 10 (2013) 221.
[10] E. Arganda, M. J. Herrero, X. Marcano, and C. Weiland, Phys. Rev. D **91**, 015001 (2015).
[11] A. G. Hessler, A. Ibarra, E. Molinaro, and S. Vogl, Phys. Rev. D **91**, 115004 (2015).
[12] M. D. Campos, A. E. C. Hernández, H. Päs, and E. Schumacher, Phys. Rev. D **91**, 116011 (2015).
[13] J. Heeck, M. Holthausen, W. Rodejohann, and Y. Shimizu, Nucl. Phys. **B896**, 281 (2015).
[14] S. Antusch and O. Fischer, J. High Energy Phys. 05 (2015) 053.
[15] R. Dermisek, E. Lunghi, and S. Shin, J. High Energy Phys. 08 (2015) 126.
[16] A. Maiezza, M. Nemevšek, and F. Nesti, Phys. Rev. Lett. **115**, 081802 (2015).
[17] T. Kobayashi, Y. Omura, F. Takayama, and D. Yasuhara, J. High Energy Phys. 10 (2015) 042.
[18] C. Bonilla, J. C. Romao, and J. W. F. Valle, New J. Phys. **18**, 033033 (2016).
[19] D. Buttazzo, G. Degrassi, P. P. Giardino, G. F. Giudice, F. Sala, A. Salvio, and A. Strumia, J. High Energy Phys. 12 (2013) 089.
[20] J. A. Casas, V. Di Clemente, A. Ibarra, and M. Quiros, Phys. Rev. D **62**, 053005 (2000).
[21] I. Gogoladze, N. Okada, and Q. Shafi, Phys. Lett. B **668**, 121 (2008).
[22] J. Elias-Miro, J. R. Espinosa, G. F. Giudice, G. Isidori, A. Riotto, and A. Strumia, Phys. Lett. B **709**, 222 (2012).
[23] B. He, N. Okada, and Q. Shafi, Phys. Lett. B **716**, 197 (2012).
[24] W. Rodejohann and H. Zhang, J. High Energy Phys. 06 (2012) 022.
[25] J. Chakrabortty, M. Das, and S. Mohanty, Mod. Phys. Lett. A **28**, 1350032 (2013).
[26] I. Masina, Phys. Rev. D **87**, 053001 (2013).
[27] W. Chao, M. Gonderinger, and M. J. Ramsey-Musolf, Phys. Rev. D **86**, 113017 (2012).
[28] S. Khan, S. Goswami, and S. Roy, Phys. Rev. D **89**, 073021 (2014).
[29] P. S. B. Dev, D. K. Ghosh, N. Okada, and I. Saha, J. High Energy Phys. 03 (2013) 150; 05 (2013) 049.
[30] S.-Y. Ho and J. Tandean, Phys. Rev. D **87**, 095015 (2013).
[31] A. Kobakhidze and A. Spencer-Smith, J. High Energy Phys. 08 (2013) 036.
[32] A. Datta, A. Elsayed, S. Khalil, and A. Moursy, Phys. Rev. D **88**, 053011 (2013).
[33] J. Chakrabortty, P. Konar, and T. Mondal, Phys. Rev. D **89**, 056014 (2014).
[34] R. N. Mohapatra and Y. Zhang, J. High Energy Phys. 06 (2014) 072.
[35] Y. Hamada, H. Kawai, and K.-y. Oda, J. High Energy Phys. 07 (2014) 026.
[36] G. Bambhaniya, S. Goswami, S. Khan, P. Konar, and T. Mondal, Phys. Rev. D **91**, 075007 (2015).
[37] G. Bambhaniya, S. Khan, P. Konar, and T. Mondal, Phys. Rev. D **91**, 095007 (2015).
[38] A. Salvio, Phys. Lett. B **743**, 428 (2015).
[39] L. Delle Rose, C. Marzo, and A. Urbano, J. High Energy Phys. 12 (2015) 050.
[40] M. Lindner, H. H. Patel, and B. Radovčić, Phys. Rev. D **93**, 073005 (2016).
[41] N. Haba, H. Ishida, N. Okada, and Y. Yamaguchi, Eur. Phys. J. C **76**, 333 (2016).
[42] F. Vissani, Phys. Rev. **D57**, 7027 (1998).
[43] J. A. Casas, J. R. Espinosa, and I. Hidalgo, J. High Energy Phys. 11 (2004) 057.
[44] A. Abada, C. Biggio, F. Bonnet, M. Gavela, and T. Hambye, J. High Energy Phys. 12 (2007) 061.
[45] M. Farina, D. Pappadopulo, and A. Strumia, J. High Energy Phys. 08 (2013) 022.
[46] J. D. Clarke, R. Foot, and R. R. Volkas, Phys. Rev. D **91**, 073009 (2015).
[47] M. Fabbrichesi and A. Urbano, Phys. Rev. D **92**, 015028 (2015).
[48] J. D. Clarke, R. Foot, and R. R. Volkas, Phys. Rev. D **92**, 033006 (2015).
[49] M. Chabab, M. C. Peyranère, and L. Rahili, Phys. Rev. D **93**, 115021 (2016).
[50] J. D. Clarke and P. Cox, J. High Energy Phys. 02 (2017) 129.
[51] A. Salvio, Phys. Rev. D **94**, 096007 (2016).
[52] P. Minkowski, Phys. Lett. B **67B**, 421 (1977).
[53] R. N. Mohapatra and G. Senjanovic, Phys. Rev. Lett. **44**, 912 (1980).
[54] T. Yanagida, Conference Proceedings **C7902131**, 95 (1979).
[55] M. Gell-Mann, P. Ramond, and R. Slansky, Conference Proceedings **C790927**, 315 (1979).
[56] S. Glashow, NATO Adv. Study Inst. Ser. B Phys. **59**, 687 (1980).
[57] A. Yu. Smirnov, Phys. Rev. D **48**, 3264 (1993).
[58] E. Ma, D. P. Roy, and U. Sarkar, Phys. Lett. B **444**, 391 (1998).
[59] S. F. King, J. High Energy Phys. 09 (2002) 011.
[60] R. Kuchimanchi and R. N. Mohapatra, Phys. Lett. B **552**, 198 (2003).
[61] P. H. Frampton, S. L. Glashow, and T. Yanagida, Phys. Lett. B **548**, 119 (2002).
[62] M. Raidal and A. Strumia, Phys. Lett. B **553**, 72 (2003).
[63] S. Raby, Phys. Lett. B **561**, 119 (2003).
[64] B. Dutta and R. N. Mohapatra, Phys. Rev. D **68**, 056006 (2003).
[65] A. Ibarra and G. G. Ross, Phys. Lett. B **591**, 285 (2004).
[66] A. Ibarra, J. High Energy Phys. 01 (2006) 064.
[67] W.-l. Guo, Z.-z. Xing, and S. Zhou, Int. J. Mod. Phys. E **16**, 1 (2007).
[68] J. Casas and A. Ibarra, Nucl. Phys. **B618**, 171 (2001).
[69] J. Schechter and J. W. F. Valle, Phys. Rev. D **25**, 774 (1982).
[70] J. G. Korner, A. Pilaftsis, and K. Schilcher, Phys. Rev. D **47**, 1080 (1993).
[71] W. Grimus and L. Lavoura, J. High Energy Phys. 11 (2000) 042.

[72] H. Hettmansperger, M. Lindner, and W. Rodejohann, J. High Energy Phys. 04 (2011) 123.
[73] S. Khan, Nucl. Phys. **B864**, 38 (2012).
[74] P. S. B. Dev and A. Pilaftsis, Phys. Rev. D **86**, 113001 (2012).
[75] D. Forero, M. Tortola, and J. Valle, Phys. Rev. D **90**, 093006 (2014).
[76] S. R. Coleman, Phys. Rev. D **15**, 2929 (1977).
[77] J. Callan, G. Curtis, and S. R. Coleman, Phys. Rev. D **16**, 1762 (1977).
[78] G. Isidori, G. Ridolfi, and A. Strumia, Nucl. Phys. **B609**, 387 (2001).
[79] J. Espinosa, G. Giudice, and A. Riotto, J. Cosmol. Astropart. Phys. 05 (2008) 002.
[80] P. A. R. Ade *et al.* (Planck Collaboration), Astron. Astrophys. **594**, A13 (2016).
[81] A. Ilakovac and A. Pilaftsis, Nucl. Phys. **B437**, 491 (1995).
[82] D. Tommasini, G. Barenboim, J. Bernabeu, and C. Jarlskog, Nucl. Phys. **B444**, 451 (1995).
[83] D. Dinh, A. Ibarra, E. Molinaro, and S. Petcov, J. High Energy Phys. 08 (2012) 125.
[84] A. M. Baldini *et al.* (MEG Collaboration), Eur. Phys. J. C **76**, 434 (2016).
[85] W. Rodejohann, Int. J. Mod. Phys. E **20**, 1833 (2011).
[86] A. Ibarra, E. Molinaro, and S. Petcov, J. High Energy Phys. 09 (2010) 108.
[87] V. Tello, M. Nemevsek, F. Nesti, G. Senjanovic, and F. Vissani, Phys. Rev. Lett. **106**, 151801 (2011).
[88] M. Mitra, G. Senjanovic, and F. Vissani, Nucl. Phys. **B856**, 26 (2012).
[89] J. Chakrabortty, H. Z. Devi, S. Goswami, and S. Patra, J. High Energy Phys. 08 (2012) 008.
[90] P. S. B. Dev, S. Goswami, M. Mitra, and W. Rodejohann, Phys. Rev. D **88**, 091301 (2013).
[91] P. S. B. Dev, S. Goswami, and M. Mitra, Phys. Rev. D **91**, 113004 (2015).
[92] Z.-z. Xing, Phys. Lett. B **679**, 255 (2009).
[93] W. Rodejohann, Phys. Lett. B **684**, 40 (2010).
[94] J. Lopez-Pavon, E. Molinaro, and S. T. Petcov, J. High Energy Phys. 11 (2015) 030.
[95] F. F. Deppisch, P. S. B. Dev, and A. Pilaftsis, New J. Phys. **17**, 075019 (2015).
[96] S. Goswami, S. Khan, and S. Mishra, Int. J. Mod. Phys. A **29**, 1450114 (2014).
[97] S. Antusch, J. Kersten, M. Lindner, and M. Ratz, Nucl. Phys. **B674**, 401 (2003).
[98] S. Antusch, J. Kersten, M. Lindner, M. Ratz, and M. A. Schmidt, J. High Energy Phys. 03 (2005) 024.
[99] M. Fukugita and T. Yanagida, Phys. Lett. **174B**, 45 (1986).
[100] S. Davidson and A. Ibarra, Phys. Lett. B **535**, 25 (2002).
[101] G. F. Giudice, A. Notari, M. Raidal, A. Riotto, and A. Strumia, Nucl. Phys. **B685**, 89 (2004).
[102] M. Flanz, E. A. Paschos, U. Sarkar, and J. Weiss, Phys. Lett. B **389**, 693 (1996).
[103] A. Pilaftsis, Phys. Rev. D **56**, 5431 (1997).
[104] A. Pilaftsis and T. E. J. Underwood, Nucl. Phys. **B692**, 303 (2004).
[105] R. G. Felipe, F. R. Joaquim, and B. M. Nobre, Phys. Rev. D **70**, 085009 (2004).
[106] K. Turzynski, Phys. Lett. B **589**, 135 (2004).
[107] G. C. Branco, R. Gonzalez Felipe, F. R. Joaquim, and B. M. Nobre, Phys. Lett. B **633**, 336 (2006).
[108] A. Pilaftsis and T. E. J. Underwood, Phys. Rev. D **72**, 113001 (2005).
[109] F. F. Deppisch and A. Pilaftsis, Phys. Rev. D **83**, 076007 (2011).
[110] P. S. B. Dev, P. Millington, A. Pilaftsis, and D. Teresi, Nucl. Phys. **B886**, 569 (2014).
[111] P. S. B. Dev, P. Millington, A. Pilaftsis, and D. Teresi, Nucl. Phys. **B897**, 749 (2015).
[112] P. S. B. Dev, P. Millington, A. Pilaftsis, and D. Teresi, Nucl. Phys. **B891**, 128 (2015).
[113] E. K. Akhmedov, V. A. Rubakov, and A. Yu. Smirnov, Phys. Rev. Lett. **81**, 1359 (1998).
[114] L. Canetti, M. Drewes, T. Frossard, and M. Shaposhnikov, Phys. Rev. D **87**, 093006 (2013).
[115] B. Shuve and I. Yavin, Phys. Rev. D **89**, 075014 (2014).
[116] W. Buchmuller, P. Di Bari, and M. Plumacher, Ann. Phys. (Berlin) **315**, 305 (2005).
[117] J. M. Cline, K. Kainulainen, and K. A. Olive, Phys. Rev. D **49**, 6394 (1994).
[118] M. D'Onofrio, K. Rummukainen, and A. Tranberg, J. High Energy Phys. 08 (2012) 123.